the free ligand exchanges rapidly on the NMR time scale with the isocyanide trans to chloride but not with the mutually trans isocyanide ligands. This phenomenon demonstrates that the kinetic trans effect of *tert*-butyl isocyanide is less than that of chloride ion. Such a result is not expected from the trans-effect series of the platinum metals, although it is in accord with the relative CO labilizing abilities of chloride ion and phenyl isocyanide in $M(CO)_5A$ complexes.[17]

The ligand-exchange properties of the isocyanide ligands were demonstrated chemically by the reaction of **2** with terpyridine to produce the known compound VCl_3(terpy).[6] The product was identified by its visible (mull) spectrum, its infrared spectrum, and elemental analysis.

A second derivative of **2** was isolated from its reaction with excess *tert*-butyl isocyanide in ethanol. The yellow compound, obtained as the hexafluorophosphate salt, was also prepared directly from vanadium(III) chloride. It is formulated as the homoleptic vanadium(II) isocyanide complex $[V(CN\text{-}t\text{-}Bu)_6](PF_6)_2$ on the basis of its elemental analysis and the presence of a C≡N absorption band at 2190 cm^{-1} in its infrared spectrum.[18]

Acknowledgment. We are grateful to the National Science Foundation for support of this work under Grant NSF CHE79 12436 and Dr. P. W. R. Corfield for valuable discussions.

Registry No. **2**, 74562-45-1; VCl_3(terpy), 64347-78-0; $[V(CN\text{-}t\text{-}Bu)_6](PF_6)_2$, 74552-65-1.

Supplementary Material Available: Table S1 listing observed and calculated structure factor amplitudes (4 pages). Ordering information is given on any current masthead page.

(17) Angelici, R. J. *Organomet. Chem. Rev., Sect. A* **1968**, *3*, 173.

(18) The hexakis(*tert*-butyl isocyanide)vanadium(II) cation has now been crystallographically characterized in the compound $[V(CN\text{-}t\text{-}Bu)_6][V(CO)_6]_2$ (Silverman, L. D.; Corfield, P. W. R.; Lippard, S. J., to be submitted for publication).

Contribution from the Department of Chemistry, San Francisco State University, San Francisco, California 94132

Entropy, Enthalpy, and Side-Arm Porphyrins. 2. Crystal and Molecular Structure of a 5-Coordinate Zinc Porphyrin with a Four-Atom Chain Attaching the Pyridyl Ligand to the Tetraphenylporphyrin

MICHAEL A. BOBRIK* and F. ANN WALKER*[1]

Received November 13, 1979

The crystal and molecular structure of $ZnTPP\text{–}NHC(O)(CH_2)_2C_5H_4N\cdot C_6H_6\cdot{}^1/_2CH_3CH_2OH$, a 5-coordinate zinc porphyrin with a covalently attached axial pyridine ligand, has been determined. The compound crystallizes in the monoclinic system, space group $P2_1/c$ (C_{2h}^5), with a = 13.970 (4) Å, b = 15.184 (6) Å, c = 26.110 (8) Å, and β = 121.54 (2)° for a cell volume of 4720 (6) Å^3 and Z = 4. Refinement of 2372 unique reflections with $F_o^2 > 3\sigma(F_o^2)$ led to R = 0.069 and R_w = 0.086. Each unit cell contains four discrete Zn porphyrin units, four benzene solvent molecules, and two ethanol solvent molecules well removed from the zinc. The plane of the axial pyridine ligand is found to be aligned over the metal and two diagonally opposed porphyrin nitrogens. The zinc out-of-plane displacement is 0.37 Å, the average $Zn\text{–}N_{por}$ distance is 2.059 Å, and the $Zn\text{–}N_{py}$ distance is 2.147(7) Å. Stability of the complex vs. bond strain and distortion, relations between solution NMR and electrochemical studies and the solid-state structure, and the orientation of the axial ligand for this and other related compounds are discussed.

Introduction

The synthesis and physicochemical investigation of a number of 5- and 6-coordinate metalloporphyrins and -chlorins in which the axial ligand(s) are covalently attached to the porphyrin ring have been reported over the past few years.[2-15] Covalent attachment of axial ligand(s) allows the coordination number and identity of axial ligand(s) to be controlled, eliminates the necessity of having excess free ligand in solution, and provides access to pure compounds of otherwise unstable coordination geometry such as 5-coordinate Fe(II) and Ni(II). Covalent attachment of axial ligands to the porphyrin ring thus allows inorganic chemists to mimic the coordination sphere of iron in the heme proteins, wherein the axial ligand(s) and coordination number are controlled by the protein residues which extend into the active site pocket. However, although covalent attachment controls coordination number and identity of axial ligands, a recent study[14] has shown that the stability

(1) Recipient, NIH Research Career Development Award, 1976–1981.
(2) V. W. Lautsch, B. Wiemer, P. Zschenderlein, H. J. Kraege, W. Bandel, D. Günther, G. Schulz, and H. Gnichtel, *Kolloid Z.*, **161**, 36 (1958).
(3) G. Losse and G. Muller, *Hoppe-Seyler's Z. Physiol. Chem.*, **327**, 205 (1962).
(4) P. K. Warme and L. P. Hager, *Biochemistry*, **9**, 1606 (1970).
(5) A. van der Heijden, H. G. Peer, and A. H. A. van den Oord, *J. Chem. Soc. D*, 369 (1971).
(6) C. K. Chang and T. G. Traylor, *Proc. Natl. Acad. Sci. U.S.A.*, **70**, 2647 (1973).
(7) C. E. Castro, *Bioinorg. Chem.*, **4**, 45 (1974).
(8) E. Bayer and G. Holzbach, *Angew. Chem., Int. Ed. Engl.*, **16**, 117 (1977).
(9) J. P. Collman, *Acc. Chem. Res.*, **10**, 265 (1977).
(10) F. S. Molinaro, R. G. Little, and J. A. Ibers, *J. Am. Chem. Soc.*, **99**, 5628 (1977).
(11) J. Geibel, J. Cannon, D. Campbell, and T. G. Traylor, *J. Am. Chem. Soc.*, **100**, 3575 (1978).
(12) D. A. Buckingham and T. B. Rauchfuss, *J. Chem. Soc., Chem. Commun.*, 705 (1978).
(13) I. S. Denniss and J. K. Sanders, *Tetrahedron Lett.*, 295 (1978).
(14) F. A. Walker and M. Benson, *J. Am. Chem. Soc.*, **102**, 5330 (1980).
(15) T. Mashiko, J.-C. Marchon, D. T. Musser, C. A. Reed, M. E. Kastner, and W. R. Scheidt, *J. Am. Chem. Soc.*, **101**, 3653 (1979).

0020-1669/80/1319-3383$01.00/0

of binding covalently attached axial ligands to zinc(II) is not as great as that of free ligands of analogous structure, and another study[10] has shown that covalent attachment of the fifth ligand does not affect the stability of oxygen binding to the sixth position of a cobalt(II) porphyrin.

Although many covalently attached, axially liganded metalloporphyrins have been prepared and studied in solution, only one report has been presented of the structure of such a compound;[15] in this case the axial ligand was attached to the porphyrin by a relatively long chain, and disorder prevented a highly detailed analysis of the structure. Because of our interest in the preparation and study of 6-coordinate metalloporphyrins as models of the cytochromes *b* in which the orientation of axial ligand planes is strictly controlled,[16] the question of the effect of covalent attachment, by the shortest possible connecting chain, on the structure of metalloporphyrin–axial ligand complexes became important to us. Studies of the structures of such 5- and 6-coordinate metalloporphyrins prepared in this laboratory have thus been undertaken. The present work describes the crystal and molecular structure of the 5-coordinate porphyrin complex of [5-[2-[(2-(3-pyridyl)ethyl)carbonylamino]phenyl]-10,15,20-triphenylporphinato]zinc(II), ZnTPP–NHC(O)$(CH_2)_2C_5H_4N$ (**1**).

The crystal and molecular structure of one 4-coordinate zinc(II) porphyrin has been reported[17] and the zinc atom shown to be in the plane of the porphyrin nitrogens. In contrast, structures of several 5-coordinate zinc porphyrins[18,19] and one 5-coordinate zinc porphyrin cation radical[20] show the zinc atom to be out of the plane of the porphyrin nitrogens by 0.2–0.3 Å in the direction of the fifth ligand, and this out-of-plane geometry has been used to explain the fact that numerous studies[14,21–26] have shown that only one axial ligand can be added to zinc(II) porphyrins.

Thermodynamics of addition of a variety of axial ligands to ZnTPP[21–27] and its phenyl-substituted analogues[26] have been reported, and the electronic factors affecting complex stability have been well delineated. The recent thermodynamic study[14] of the displacement of the covalently attached 3-pyridyl side arm of **1** and several of its analogues by free 3-picoline in toluene solution pointed out that the Zn–N bond strength of the side-arm pyridyl ligand is less than that of 3-picoline, no matter what the length of the attaching chain. We were therefore interested to see if any bond strain would be apparent in the molecular structures of these compounds.

The majority of crystal and molecular structure determinations of metalloporphyrin complexes having at least one planar axial ligand (usually a pyridine or imidazole) have axial ligand plane projections on the porphyrin nitrogen axis of less than 26°,[15,18,28–40] while only six reported structures[32,41–45] have ligand plane angles near the 45° angle which places the axial ligand plane over the meso carbons of the porphyrin ring, the expected minimum energy angle with regard to electron repulsion between hydrogen atoms bound to carbons adjacent to the coordinating nitrogen of the axial ligand and the electron density of the porphyrin ring. The reasons for this may include M–L π bonding involving the d_{xz} and d_{yz} orbitals of the metal and the π and/or π^* orbitals which involve the porphyrin nitrogens, or they may include crystal packing forces.[32] In any event, one would expect, and space-fitting molecular models (CPK) suggest, that the covalent attachment of an axial ligand to an ortho position of a phenyl group of tetraphenylporphyrin, as in compound **1**, if the attaching chain is short, should encourage the axial ligand plane to stay close to the 45° angle. One of the purposes of the present work is to test this hypothesis.

Table I. Summary of Crystal Data, Intensity Collection, and Structure Solution and Refinement for ZnTPP–NHC(O)$CH_2CH_2C_6H_4N\cdot C_6H_6\cdot{}^1/_2C_2H_5OH$

formula	$ZnO_{1.5}N_6C_{59}H_{45}$
a, Å	13.970 (4)[a]
b, Å	15.184 (6)
c, Å	26.110 (8)
β, deg	121.54 (2)
V, Å^3	4720 (6)
Z	4
d_{calcd} (d_{obsd}), g cm^{-3}	1.27 (1.30)[b]
space group	$P2_1/c$
cryst dimens, mm^3	0.4 × 0.3 × 0.25[c]
radiation[d]	Mo ($\lambda(K\alpha)$ = 0.710 69 Å)
abs coeff, μ, cm^{-1}	5.96[e]
takeoff angle, deg	3.0
scan speed, deg min^{-1}	1.5–29.3 (θ–2θ scan)
scan range, deg	0.8 below $K\alpha_1$ to 0.8 above $K\alpha_2$
bkgd counts	bkgd/scan time = 0.25
2θ limit, deg	40.0
phasing technique	heavy atom
unique data ($F_o^2 > 3\sigma(F_o^2)$)	2372
no. of variables (last cycle)	487
"ignorance" factor, *p*	0.05
error in observn of unit wt, e	2.29
R, %	6.9
R_w, %	8.6

[a] Here and elsewhere in this report, standard deviations are given in parentheses. [b] Determined by flotation in aqueous $ZnCl_2$. [c] Prism (V = 0.033 mm^3). [d] Mosaic graphite monochromator. [e] Gaussian numerical integration program used for absorption correction.

Experimental Section

Crystal Data for ZnTPP–NHC(O)$(CH_2)_2C_5H_4N\cdot C_6H_6\cdot{}^1/_2CH_3CH_2OH$. The zinc porphyrin under study, ZnTPP–NHC(O)$(CH_2)_2C_5H_4N$ (**1**), was synthesized and purified as described

(16) F. A. Walker, manuscript in preparation.
(17) W. R. Scheidt, M. E. Kastner, and K. Hatano, *Inorg. Chem.*, **17**, 706 (1978).
(18) M. D. Glick, G. H. Cohen, and J. L. Hoard, *J. Am. Chem. Soc.*, **89**, 1996 (1967).
(19) D. M. Collins and J. L. Hoard, *J. Am. Chem. Soc.*, **92**, 3761 (1970).
(20) L. D. Spaulding, P. G. Eller, J. A. Bertrand, and R. H. Felton, *J. Am. Chem. Soc.*, **96**, 982 (1974).
(21) J. R. Miller and G. D. Dorough, *J. Am. Chem. Soc.*, **74**, 3977 (1952).
(22) C. H. Kirksey, P. Hambright, and C. B. Storm, *Inorg. Chem.*, **8**, 2141 (1969).
(23) S. J. Cole, G. C. Curthoys, E. A. Magnusson, and J. N. Phillips, *Inorg. Chem.*, **11**, 1024 (1972).
(24) G. C. Vogel and L. A. Searby, *Inorg. Chem.*, **12**, 936 (1973).
(25) G. C. Vogel and B. A. Beckmann, *Inorg. Chem.*, **15**, 483 (1976).
(26) G. C. Vogel and J. R. Stahlbush, *Inorg. Chem.*, **16**, 950 (1977).
(27) M. Nappa and J. S. Valentine, *J. Am. Chem. Soc.*, **100**, 5075 (1978).
(28) J. F. Kirner, C. A. Reed, and W. R. Scheidt, *J. Am. Chem. Soc.*, **99**, 2557 (1977).
(29) D. M. Collins, R. Countryman, and J. L. Hoard, *J. Am. Chem. Soc.*, **94**, 2066 (1972).
(30) R. G. Little, K. R. Dymock, and J. A. Ibers, *J. Am. Chem. Soc.*, **97**, 4532 (1975).
(31) A. Takenaka, Y. Sasada, F. Watanabe, H. Ogoshi, and Z. Yoshida, *Chem. Lett.*, 1235 (1972).
(32) J. L. Hoard, private communication.
(33) R. G. Little and J. A. Ibers, *J. Am. Chem. Soc.*, **95**, 8583 (1973).
(34) W. R. Scheidt and P. L. Piciulo, *J. Am. Chem. Soc.*, **98**, 1913 (1976).
(35) W. R. Scheidt, *J. Am. Chem. Soc.*, **96**, 90 (1974).
(36) R. G. Little and J. A. Ibers, *J. Am. Chem. Soc.*, **96**, 4452 (1974).
(37) P. N. Dwyer, P. Madura, and W. R. Scheidt, *J. Am. Chem. Soc.*, **96**, 4815 (1974).
(38) R. G. Little and J. A. Ibers, *J. Am. Chem. Soc.*, **96**, 4440 (1974).
(39) G. B. Jameson, G. A. Rodley, W. T. Robinson, R. R. Gagne, C. A. Reed, and J. P. Collman, *Inorg. Chem.*, **17**, 850 (1978).
(40) K. M. Adams, P. G. Rasmussen, W. R. Scheidt, and K. Hatano, *Inorg. Chem.*, **18**, 1892 (1979).
(41) J. F. Kirner, J. Garofalo, and W. R. Scheidt, *Inorg. Nucl. Chem. Lett.*, **11**, 107 (1975).
(42) S.-M. Peng and J. A. Ibers, *J. Am. Chem. Soc.*, **98**, 8032 (1976).
(43) J. W. Lauher and J. A. Ibers, *J. Am. Chem. Soc.*, **96**, 4447 (1974).
(44) J. A. Kaduk and W. R. Scheidt, *Inorg. Chem.*, **13**, 1875 (1974).
(45) W. R. Scheidt and J. A. Ramanuja, *Inorg. Chem.*, **14**, 2643 (1975).

previously.[14] Simple evaporation of, or recrystallization from, toluene and benzene solutions of **1** yielded only flakelike crystals unsuitable for X-ray analysis. A few usable crystals were obtained by solvent diffusion, under N_2, in the dark, of absolute ethanol into a saturated benzene solution of the porphyrin. It was subsequently found (vide infra) that **1**, as crystallized, contained one C_6H_6 molecule and a half molecule of EtOH per Zn porphyrin unit. Consequently, those crystals were subjected to elemental analysis. Anal. Calcd for $C_{52}H_{36}N_6OZn \cdot C_6H_6 \cdot {}^1/_2CH_3CH_2OH$: C, 76.41; H, 4.89; N, 9.06; O, 2.59; Zn, 7.06. Found: C, 76.79; H, 5.05; N, 8.95; O, 2.32 (by difference); Zn, 6.90. Calcd for $C_{52}H_{36}N_6OZn \cdot C_6H_6$ (for comparison): C, 77.03; H, 4.68; N, 9.29; O, 1.77; Zn, 7.23.

Diffraction studies were carried out on a Syntex $P2_1$ four-circle automated diffractometer at the Department of Chemistry, Stanford University. Crystals were epoxied to the end of glass fibers for mounting on the diffractometer. That one crystal which diffracted best was used in subsequent work. Machine centering of 15 reflections with 2θ values in the range of 3.0–12.0° yielded initial approximate cell dimensions. Axial photographs showed $2/m$ diffraction symmetry, confirming that the crystal was indeed of the monoclinic system. A short data collection produced 15 reflections in the 2θ range of 9.3–20.6° of intensity sufficient for machine recentering. Least-squares refinement based on these reflections gave the orientation matrix and cell parameter esd's. ω scans of six low angle reflections had symmetric, single peaks with widths at half-height less than 0.3°, indicating suitable mosaicity and no twinning. Crystal data are summarized in Table I.

Data Collection and Reduction. The parameters and conditions employed in data collection are presented in Table I. During the course of data collection, standards (104, 100, and 020) were collected every 60 reflections. Both a slight decay (ca. 7%) and a significant instability in the X-ray power supply were evident from inspection of the standards. These fluctuations were corrected for by using the Stanford program CHORTA.[46] Otherwise, data were processed as described previously.[47,48] Inspection of intensities unambiguously determined the space group to be $P2_1/c$ (C_{2h}^5). Of the 5643 reflections originally collected, 2372 reflections were used in refinement after rejecting systematic absences, symmetry-redundant data, and those reflections with $F^2 < 3\sigma(F^2)$. The data set used in the final stages of refinement was further corrected for absorption by using a Gaussian numerical integration program.

Structure Solution and Refinement. A Patterson function clearly yielded Harker sections from which the Zn atom was located. An initial difference Fourier map, phased only with the metal, located the five nitrogen atoms. Subsequent cycles of refinement and difference maps gave positions for the porphyrin, a molecule of benzene solvate, and a molecule of ethanol, refined with half-occupancy, located near the origin. The statistical weighting scheme used in the full-matrix least-squares refinement has been reported previously.[47]

The course of refinement was as follows (values of R and R_w in parentheses): Zn and porphine core, isotropic (35.0, 45.0); all nonhydrogen and nonsolvent atoms, isotropic (16.4, 23.4); all nonhydrogen atoms, isotropic (13.5, 17.4). In the final sets of refinement cycles, the zinc, the porphine core atoms, the pyridine, the covalent linkage, and the phenyl group to which it is attached were refined anisotropically. Other nonhydrogen atoms were refined isotropically. All parameters converged to unique values, and all anisotropic temperature factors remained positive-definite throughout the refinement. H atoms were included for the porphyrin portion of the molecule; their positions were generated with the assumption of C–H distances of 1.0 Å, and their isotropic temperature factors set at 1 greater than the atom to which they were attached. H atoms were not refined. Due to distortion and disorder of the solvent molecules, no H atoms were included for these. The hydrogen bonded to the amide nitrogen of the covalent linkage could not be unambiguously located from the final difference Fourier map. The final cycle converged to $R = 6.9\%$, $R_w = 8.6\%$, and the final error in an observation of unit weight was 2.29 electrons. The highest peak in the final difference Fourier map was approximately 15% of the height of a carbon atom in previous maps and represented an electron density of 0.26 e/Å^3. The highest shift/error ratio in the last refinement cycle was 0.21 for the solvent molecules and 0.04 for the porphyrin.

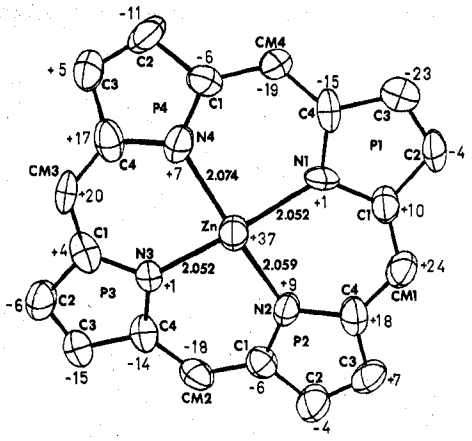

Figure 1. The porphine core of **1** viewed approximately down the crystallographic c axis. The atomic numbering scheme and deviations (in 0.01 Å units) from the plane of the porphyrin ring are shown.

The following information is presented in table form: positional and thermal parameters, Table II; bond distances and angles, Tables III and IV; best weighted least-squares planes, Table V; root-mean-square amplitudes of thermal vibration, Table VI. Given elsewhere[49] are calculated hydrogen positions (Table VII), general temperature factor expressions, B's and U's (Table VIII), and values of $10|F_o|$ and $10|F_c|$ (Table IX).

Results

The cell contents consist of well-separated enantiomeric Zn porphyrin units, as well as benzene and ethanol molecules of crystallization. During refinement and structure solution, a difference Fourier map clearly revealed a six-membered ring, attributed to solvent benzene, located closest to the covalent side arm to which the axial pyridine is attached. (The closest contact is between a carbon of the benzene (C6B) and H29 of the side arm–2.98 Å.) This may be contrasted with several metalloporphyrin–toluene solvate structures in which the aryl solvent is located within 3.6 Å of the metal and is roughly parallel to the porphyrin plane.[17,50,51]

Near the end of structure solution it became evident that there was still considerable electron density near the origin in difference maps. Three peaks were consistently found situated in such a way as to be treated as an ethanol molecule. In $P2_1/c$ the origin is a special position of inversion symmetry. To include one CH_3CH_2OH unit per porphyrin would have required unreasonably close contacts between inversion-related ethanols. Hence this solvent was refined with half-occupancies assigned to the two carbons and the oxygen. The methyl and hydroxyl groups were distinguished by the behavior of their thermal parameters during subsequent refinement. Elemental analysis of that crop of crystals from which the one studied was obtained confirmed the stoichiometry imposed by inclusion of a half ethanol molecule per Zn porphyrin.

Refinement of the ethanol, however, unfortunately led to unacceptable values for the interatomic distances and included angle. It is concluded that the alcohol is very much disordered, perhaps rotationally about the C–C and/or C–O vectors. This disorder most likely contributes to the rather high values of the residuals and the distance and angle esd's. The positional

(46) Stanford University's local program for correction of anisotropic crystal decay.
(47) M. A. Bobrik, K. O. Hodgson, and R. H. Holm, *Inorg. Chem.*, **16**, 1851 (1977).
(48) Stanford programs include data reduction, full-matrix least-squares, and Fourier local programs, a modified version of Busing and Levy's function and error program ORFFE, as well as Johnson's ORTEP. A PDP 11/45 computer was used to carry out the calculations. Atomic scattering factors used were from "International Tables for X-ray Crystallography", Vol. IV, Kynoch Press, Birmingham, England, 1974.
(49) Supplementary material.
(50) J. F. Kirner, C. A. Reed, and W. R. Scheidt, *J. Am. Chem. Soc.*, **99**, 1093 (1977).
(51) W. R. Scheidt and C. A. Reed, *Inorg. Chem.*, **17**, 710 (1978).

Table II. Positional and Thermal Parameters for ZnTPP-NHC(O)$CH_2CH_2C_6H_4N\cdot C_6H_6\cdot{}^1/_2C_2H_5OH$ (Nonhydrogen Atoms Only)

atom	x	y	z	β_{11}[a]	β_{22}	β_{33}	β_{12}	β_{13}	β_{23}
Zn	0.1630 (1)	0.04093 (9)	0.34753 (5)	0.00710 (7)	0.00288 (6)	0.00200 (2)	−0.0002 (2)	0.00400 (6)	−0.00017 (9)
O1S	0.5447 (7)	0.326 (1)	0.4476 (4)	0.0213 (8)	0.026 (1)	0.0080 (3)	0.027 (2)	0.0211 (6)	0.0180 (9)
N1	0.0885 (5)	0.1570 (6)	0.3482 (3)	0.0063 (5)	0.0041 (5)	0.0025 (2)	0.0011 (9)	0.0066 (4)	0.0003 (5)
N2	0.2409 (6)	0.1088 (5)	0.3110 (3)	0.0057 (6)	0.0024 (5)	0.0018 (2)	−0.0013 (9)	0.0026 (4)	−0.0002 (5)
N3	0.1917 (6)	−0.0732 (5)	0.3156 (3)	0.0064 (6)	0.0025 (5)	0.0022 (2)	0.0003 (8)	0.0046 (4)	0.0002 (5)
N4	0.0464 (6)	−0.0265 (6)	0.3590 (3)	0.0073 (6)	0.0029 (5)	0.0022 (2)	−0.002 (1)	0.0038 (5)	−0.0003 (5)
N5	0.2979 (6)	0.0476 (6)	0.4397 (3)	0.0088 (6)	0.0038 (5)	0.0018 (2)	0.001 (1)	0.0034 (5)	0.0002 (6)
N1S	0.3825 (8)	0.3370 (7)	0.4442 (4)	0.0083 (8)	0.0056 (7)	0.0030 (3)	−0.001 (1)	0.0006 (7)	0.0001 (7)
C1P1	0.1253 (8)	0.2399 (7)	0.3450 (4)	0.0091 (8)	0.0025 (6)	0.0020 (2)	−0.001 (1)	0.0054 (6)	−0.0004 (6)
C2P1	0.0600 (8)	0.3037 (7)	0.3551 (5)	0.0115 (9)	0.0021 (6)	0.0033 (3)	−0.002 (1)	0.0077 (6)	−0.0020 (7)
C3P1	−0.0128 (8)	0.2596 (8)	0.3628 (5)	0.0090 (8)	0.0050 (7)	0.0033 (3)	0.000 (1)	0.0076 (6)	−0.0005 (7)
C4P1	0.0062 (8)	0.1672 (7)	0.3607 (4)	0.0084 (8)	0.0018 (6)	0.0016 (2)	0.001 (1)	0.0024 (6)	0.0002 (6)
C1P2	0.2974 (7)	0.0744 (7)	0.2860 (4)	0.0066 (7)	0.0036 (6)	0.0016 (2)	0.000 (1)	0.0036 (6)	−0.0007 (6)
C2P2	0.3485 (8)	0.1435 (8)	0.2710 (5)	0.0129 (8)	0.0043 (7)	0.0038 (3)	−0.002 (1)	0.0107 (6)	−0.0002 (7)
C3P2	0.3246 (8)	0.2195 (8)	0.2884 (4)	0.0094 (8)	0.0047 (7)	0.0030 (2)	−0.003 (1)	0.0078 (6)	0.0003 (7)
C4P2	0.2554 (8)	0.1988 (7)	0.3136 (4)	0.0079 (8)	0.0026 (6)	0.0021 (2)	0.001 (1)	0.0032 (6)	0.0003 (7)
C1P3	0.1627 (8)	−0.1570 (7)	0.3237 (4)	0.0092 (8)	0.0034 (6)	0.0011 (2)	0.003 (1)	0.0034 (6)	0.0002 (6)
C2P3	0.2117 (8)	−0.2216 (7)	0.3034 (5)	0.0084 (9)	0.0032 (6)	0.0024 (2)	−0.002 (1)	0.0037 (7)	−0.0007 (7)
C3P3	0.2682 (8)	−0.1764 (8)	0.2841 (5)	0.0097 (8)	0.0032 (6)	0.0036 (3)	0.001 (1)	0.0072 (7)	−0.0007 (7)
C4P3	0.2540 (8)	−0.0842 (7)	0.2901 (4)	0.0083 (8)	0.0029 (6)	0.0017 (2)	0.000 (1)	0.0037 (6)	−0.0002 (6)
C1P4	−0.0280 (7)	0.0094 (7)	0.3719 (4)	0.0059 (7)	0.0042 (7)	0.0024 (2)	0.002 (1)	0.0047 (5)	0.0006 (6)
C2P4	−0.0789 (8)	−0.0618 (8)	0.3854 (4)	0.0083 (7)	0.0048 (7)	0.0029 (2)	−0.003 (1)	0.0065 (6)	0.0011 (7)
C3P4	−0.0385 (8)	−0.1377 (8)	0.3797 (5)	0.0087 (8)	0.0029 (6)	0.0038 (3)	−0.002 (1)	0.0062 (7)	−0.0005 (8)
C4P4	0.0444 (8)	−0.1157 (7)	0.3644 (4)	0.0055 (8)	0.0028 (6)	0.0020 (3)	0.001 (1)	0.0004 (7)	−0.0001 (7)
CM1	0.2062 (8)	0.2610 (7)	0.3321 (4)	0.0085 (8)	0.0032 (6)	0.0022 (2)	−0.002 (1)	0.0053 (5)	0.0005 (6)
CM2	0.3043 (8)	−0.0154 (8)	0.2758 (4)	0.0075 (7)	0.0045 (7)	0.0023 (2)	0.002 (1)	0.0053 (6)	−0.0003 (7)
CM3	0.1009 (8)	−0.1754 (7)	0.3496 (4)	0.0083 (8)	0.0016 (5)	0.0013 (2)	−0.002 (1)	0.0021 (6)	0.0002 (6)
CM4	−0.0488 (7)	0.0999 (7)	0.3718 (4)	0.0065 (7)	0.0034 (6)	0.0025 (2)	0.000 (1)	0.0055 (5)	0.0009 (6)
C1R1	0.2384 (7)	0.3560 (7)	0.3347 (4)	0.0070 (8)	0.0024 (6)	0.0020 (2)	−0.002 (1)	0.0038 (6)	−0.0015 (6)
C2R1	0.1807 (9)	0.4094 (8)	0.2857 (5)	0.011 (1)	0.0033 (6)	0.0026 (3)	0.002 (1)	0.0046 (7)	0.0036 (7)
C3R1	0.2135 (9)	0.4966 (8)	0.2902 (5)	0.010 (1)	0.0058 (8)	0.0026 (3)	0.006 (1)	0.0044 (7)	0.0042 (8)
C4R1	0.3023 (8)	0.5292 (8)	0.3431 (5)	0.0109 (9)	0.0033 (7)	0.0035 (3)	0.001 (1)	0.0070 (7)	0.0017 (8)
C5R1	0.3575 (9)	0.4776 (7)	0.3919 (5)	0.0096 (9)	0.0029 (7)	0.0025 (3)	−0.001 (1)	0.0030 (7)	0.0001 (7)
C6R1	0.3226 (8)	0.3911 (7)	0.3873 (4)	0.0105 (9)	0.0023 (6)	0.0020 (2)	0.003 (1)	0.0046 (6)	0.0030 (6)
C1S	0.490 (1)	0.3126 (9)	0.4692 (5)	0.010 (1)	0.0075 (9)	0.0026 (3)	0.005 (2)	0.0028 (8)	0.0039 (9)
C2S	0.541 (1)	0.2713 (9)	0.5298 (5)	0.012 (1)	0.0057 (8)	0.0022 (3)	0.003 (2)	0.0016 (9)	−0.0001 (9)
C3S	0.5688 (9)	0.1729 (8)	0.5303 (5)	0.008 (1)	0.0048 (8)	0.0024 (3)	−0.001 (2)	0.0000 (9)	−0.0007 (8)
C1PD	0.3887 (8)	0.0970 (8)	0.4574 (4)	0.0080 (8)	0.0037 (7)	0.0023 (2)	−0.002 (1)	0.0037 (6)	−0.0011 (7)
C2PD	0.4712 (8)	0.1128 (7)	0.5161 (4)	0.0061 (9)	0.0037 (6)	0.0013 (2)	−0.001 (1)	−0.0008 (7)	−0.0011 (7)
C3PD	0.458 (1)	0.0740 (9)	0.5594 (5)	0.015 (1)	0.0074 (9)	0.0009 (2)	0.001 (2)	0.0017 (8)	0.0010 (8)
C4PD	0.367 (1)	0.021 (1)	0.5430 (5)	0.014 (1)	0.009 (1)	0.0027 (3)	−0.010 (2)	0.0043 (8)	−0.0002 (9)
C5PD	0.2893 (9)	0.0100 (9)	0.4836 (5)	0.011 (1)	0.0067 (8)	0.0022 (3)	−0.005 (2)	0.0035 (7)	−0.0006 (8)

atom	x	y	z	B, Å^2	atom	x	y	z	B, Å^2
C1R2	0.3705 (8)	−0.0411 (8)	0.2479 (4)	4.8 (3)	C3R4	−0.330 (1)	0.176 (1)	0.3499 (6)	7.7 (4)
C2R2	0.4833 (9)	−0.0276 (9)	0.2766 (5)	6.6 (3)	C4R4	−0.297 (1)	0.183 (1)	0.4074 (5)	7.1 (4)
C3R2	0.545 (1)	−0.051 (1)	0.2480 (6)	8.0 (4)	C5R4	−0.196 (1)	0.166 (1)	0.4538 (6)	8.6 (4)
C4R2	0.484 (1)	−0.084 (1)	0.1935 (6)	7.7 (4)	C6R4	−0.116 (1)	0.134 (1)	0.4413 (5)	6.8 (4)
C5R2	0.378 (1)	−0.096 (1)	0.1616 (6)	8.5 (4)	C1B	0.419 (2)	0.148 (2)	0.1299 (8)	13.5 (7)
C6R2	0.315 (1)	−0.075 (1)	0.1905 (6)	7.7 (4)	C2B	0.4171 (17)	0.228 (2)	0.1538 (9)	16.8 (8)
C1R3	0.0928 (8)	−0.2722 (8)	0.3635 (4)	4.4 (3)	C3B	0.320 (2)	0.270 (2)	0.1073 (9)	15.8 (8)
C2R3	0.018 (1)	−0.3291 (9)	0.3206 (5)	6.8 (4)	C4B	0.243 (2)	0.245 (2)	0.5468 (1)	17.9 (9)
C3R3	0.009 (1)	−0.417 (1)	0.3359 (5)	6.9 (4)	C5B	0.258 (2)	0.167 (2)	0.027 (1)	20 (1)
C4R3	0.080 (1)	−0.447 (1)	0.3917 (5)	7.3 (4)	C6B	0.346 (2)	0.112 (2)	0.0718 (9)	16.3 (8)
C5R3	0.163 (1)	−0.394 (1)	0.4329 (5)	7.3 (4)	C1ET	0.972 (3)	0.888 (3)	0.979 (2)	14 (1)
C6R3	0.1665 (9)	−0.3041 (9)	0.4193 (5)	6.4 (4)	C2ET	0.088 (3)	0.028 (3)	0.049 (1)	11 (1)
C1R4	−0.1404 (8)	0.1258 (8)	0.3839 (4)	4.7 (3)	O1ET	0.063 (2)	0.559 (2)	0.532 (1)	16 (1)
C2R4	−0.2452 (9)	0.1443 (9)	0.3381 (5)	5.7 (3)					

[a] The form of the anisotropic thermal ellipsoid is $\exp[-(\beta_{11}h^2 + \beta_{22}k^2 + \beta_{33}l^2 + \beta_{12}hk + \beta_{13}hl + \beta_{23}kl)]$.

and thermal parameters presented in Table II for the ethanol atoms are those to which the structure converged during refinement; they are *not* meant to be taken as chemically reasonable positions but rather as an approximation of the electron density about the origin due to these disordered atoms.

The high thermal motion of the carbonyl oxygen (O1S) may also be indicative of a disorder of this atom about two positions. However, it was located from a single difference Fourier peak, and when the high thermal parameter was first noted, the oxygen position was reset to its original value and fixed. A difference map produced after partial structure refinement with the O1S coordinates fixed showed neglible electron density near this atom. That is, if there is some disorder in this region, a difference Fourier map did not indicate it. The high thermal parameters of the carbonyl oxygen could also be attributed to large librational motion of the planar amide group.

Figure 1 shows the atomic labeling scheme for the porphine portion of the molecule, selected bond distances, and displacements of the zinc and the porphyrin atoms from the plane defined by the porphine unit.

Figure 2 is a stereoview of the molecule. One notable difference between the present structure and those reported for other 5-coordinate zinc porphyrins[18-20] is the overall shape of the porphyrin ring. In the latter structures, all in-plane nitrogens are shifted above the plane in the direction of the axial ligand. In the current structure, those porphyrin nitrogens (N2 and N4) which are aligned with the axial ligand ring

Table III. Selected Bond Distances (Å) and Angles (Deg)[a]

Zn Coordination Sphere			
Zn-N1	2.052 (7)	Zn-N4	2.074 (7)
Zn-N2	2.059 (7)	mean	2.059
Zn-N3	2.052 (7)	Zn-N5	2.147 (7)
N-Zn-N			
N1-Zn-N2	88.1 (3)	N1-Zn-N5	95.8 (3)
N1-Zn-N4	89.0 (3)	N2-Zn-N5	97.4 (3)
N2-Zn-N3	88.4 (3)	N3-Zn-N5	104.6 (3)
N3-Zn-N4	88.7 (3)	N4-Zn-N5	99.0 (3)
mean	88.6	mean	99.2
N1-Zn-N3	159.5 (2)		
N2-Zn-N4	163.5 (2)		
mean	161.5		
Porphyrin Core			
C-N			
N1-C1P1	1.377 (10)	N3-C4P3	1.354 (10)
N1-C4P1	1.360 (10)	N4-C1P4	1.363 (10)
N2-C1P2	1.363 (10)	N4-C4P4	1.364 (10)
N2-C4P2	1.378 (10)	mean	1.368
N3-C1P3	1.385 (10)		
C-C			
C1P1-C2P1	1.447 (11)	CM1-C1P1	1.377 (11)
C3P1-C4P1	1.434 (11)	CM1-C4P2	1.396 (11)
C1P2-C2P2	1.435 (11)	CM2-C1P2	1.402 (11)
C3P2-C4P2	1.459 (11)	CM2-C4P3	1.415 (11)
C1P3-C2P3	1.447 (11)	CM3-C1P3	1.374 (11)
C3P3-C4P3	1.434 (11)	CM3-C4P4	1.382 (11)
C1P4-C2P4	1.435 (11)	CM4-C1P4	1.405 (11)
C3P4-C4P4	1.449 (12)	CM4-C4P1	1.396 (11)
mean	1.443	mean	1.393
C2P1-C3P1	1.317 (11)	CM1-C1R1	1.501 (11)
C2P2-C3P2	1.346 (11)	CM2-C1R2	1.498 (11)
C2P3-C3P3	1.329 (11)	CM3-C1R3	1.531 (11)
C2P4-C3P4	1.326 (11)	CM4-C1R4	1.522 (11)
mean	1.330	mean	1.513
C-N-C			
C1P1-N1-C4P1	107.4 (7)	C1P4-N4-C4P4	108.2 (8)
C1P2-N2-C4P2	107.2 (8)	mean	107.2
C1P3-N3-C4P3	106.1 (8)		
N-C-C			
N1-C1P1-C2P1	108.2 (8)	N1-C1P1-CM1	127.4 (9)
N1-C4P1-C3P1	108.4 (8)	N1-C4P1-CM4	126.4 (8)
N2-C1P2-C2P2	110.3 (8)	N2-C1P2-CM2	125.4 (9)
N2-C4P2-C3P2	107.9 (9)	N2-C4P2-CM1	127.0 (9)
N3-C1P3-C2P3	109.5 (9)	N3-C1P3-CM3	124.9 (9)
N3-C4P3-C3P3	109.7 (9)	N3-C4P3-CM2	125.1 (8)
N4-C1P4-C2P4	107.5 (8)	N4-C1P4-CM4	125.0 (9)
N4-C4P4-C3P4	108.6 (9)	N4-C4P4-CM3	125.3 (10)
mean	108.8	mean	125.8
C-C-C			
C1P1-C2P1-C3P1	107.3 (9)	C1P1-CM1-C4P2	122.9 (8)
C2P1-C3P1-C4P1	108.7 (9)	C1P2-CM2-C4P3	125.1 (8)
C1P2-C2P2-C3P2	106.7 (9)	C1P3-CM3-C4P4	126.9 (9)
C2P2-C3P2-C4P2	107.9 (8)	C1P4-CM4-C4P1	125.5 (8)
C1P3-C2P3-C3P3	106.2 (9)	mean	125.1
C2P3-C3P3-C4P3	108.6 (9)	CM1-C1R1-C2R1	120.8 (9)
C1P4-C2P4-C3P4	109.4 (9)	CM1-C1R1-C6R1	120.1 (9)
C2P4-C3P4-C4P4	106.2 (9)	CM2-C1R2-C2R2	121.7 (9)
mean	107.6	CM2-C1R2-C6R2	119.4 (8)
C1R1-CM1-C1P1	118.6 (9)	CM3-C1R3-C2R3	122.2 (9)
C1R1-CM1-C4P2	118.4 (8)	CM3-C1R3-C6R3	119.2 (8)
C1R2-CM2-C1P2	117.9 (10)	CM4-C1R4-C2R4	120.6 (8)
C1R2-CM2-C4P3	117.1 (9)	CM4-C1R4-C6R4	120.0 (8)
C1R3-CM3-C1P3	117.1 (10)	mean	120.5
C1R3-CM3-C4P4	116.9 (9)		
C1R4-CM4-C1P4	116.6 (8)		
C1R4-CM4-C4P1	117.9 (8)		
mean	117.6		
Side Arm and Pyridine			
Distances			
N5-C1PD	1.330 (10)	C2PD-C3S	1.517 (12)
N5-C5PD	1.341 (11)	C3S-C2S	1.543 (12)
C1PD-C2PD	1.374 (11)	C2S-C1S	1.489 (13)
C2PD-C3PD	1.368 (12)	C1S-O1S	1.181 (12)
C3PD-C4PD	1.366 (13)	C1S-N1S	1.339 (12)
C4PD-C5PD	1.361 (12)	N1S-C6R1	1.512 (11)
mean	1.367		
Angles			
C1PD-N5-C5PD	116.0 (8)	C1PD-C2PD-C3S	120.0 (10)
N5-C1PD-C2PD	125.3 (9)	C3PD-C2PD-C3S	123.3 (9)
C1PD-C2PD-C3PD	116.7 (9)	C2PD-C3S-C2S	112.9 (8)
C2PD-C3PD-C4PD	119.8 (9)	C3S-C2S-C1S	113.2 (8)
C3PD-C4PD-C5PD	119.3 (10)	C2S-C1S-O1S	120.6 (12)
C4PD-C5PD-N5	122.9 (9)	C2S-C1S-N1S	115.1 (12)
mean	120.0	O1S-C1S-N1S	124.1 (11)
		C1S-N1S-C6R1	122.3 (9)
		N1S-C6R1-C1R1	121.3 (8)
		N1S-C6R1-C5R1	116.2 (9)

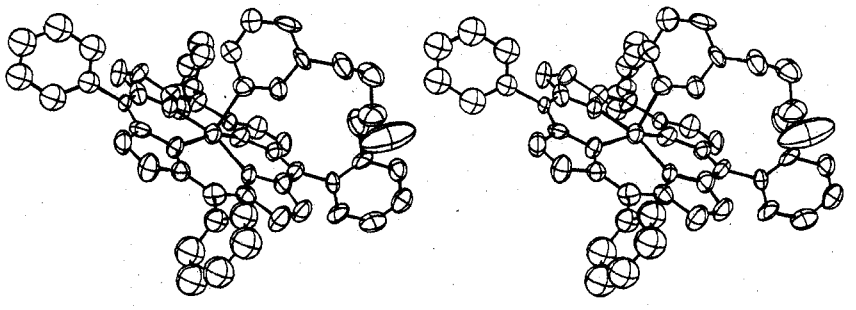

Figure 2. An ORTEP stereoview of **1**. In this and other figures 50% probability ellipsoids are presented. Hydrogen atoms are omitted.

(vide infra) are displaced above the plane; the other two nitrogens (N1 and N3) are below the plane. In addition, the porphyrin demonstrates considerable distortion from planarity, the methine carbons in particular being dislocated from the mean plane by as much as 0.24 Å. This displacement of the methine carbons results in the distinct tipping of the phenyl rings to which they are bonded relative to the porphyrin plane. The magnitude of this tipping is 6–8°; rings 1 and 3 are displaced in the direction of the axial ligand and rings 2 and 4 in the opposite direction.

The dihedral angles between the phenyl ring planes and the plane defined by the porphyrin are presented in Table V. It can be seen that this angle only significantly differs from 90° for ring 2 (69.0°)., Interestingly, this angle for ring 1 is 92.1°. Given the seemingly unfavorable orientation of the pyridine ring relative to the porphyrin nitrogens, one might have expected a considerable twisting of the phenyl group around the CM1–C1R1 vector to accommodate the conformation of the covalent linkage.

The zinc in this molecule is strictly 5-coordinate. In contrast to previously reported aryl[17,50,51] and alcohol[52] solvates of

(52) P. Gans, G. Buisson, E. Duée, J.-R. Regnard, and J.-C. Marchon, *J. Chem. Soc., Chem. Commun.* 393 (1979).

Table IV. Bond Distances (Å) and Angles (Deg) for Phenyl Groups and Solvent Molecules[a]

C1R1–C2R1	1.367 (11)	C1R3–C2R3	1.368 (11)
C2R1–C3R1	1.385 (12)	C2R3–C3R3	1.416 (13)
C3R1–C4R1	1.378 (12)	C3R3–C4R3	1.339 (12)
C4R1–C5R1	1.344 (11)	C4R3–C5R3	1.355 (12)
C5R1–C6R1	1.384 (11)	C5R3–C6R3	1.418 (13)
C6R1–C1R1	1.364 (11)	C6R3–C1R3	1.360 (11)
C1R1–C2R2	1.361 (11)	C1R4–C2R4	1.349 (10)
C2R2–C3R2	1.446 (12)	C2R4–C3R4	1.450 (12)
C3R2–C4R2	1.319 (12)	C3R4–C4R4	1.324 (12)
C4R2–C5R2	1.280 (12)	C4R4–C5R4	1.314 (12)
C5R2–C6R2	1.455 (13)	C5R4–C6R4	1.409 (13)
C6R2–C1R2	1.380 (11)	C6R4–C1R4	1.357 (11)
		mean	1.372
C1R1–C2R1–C3R1	118.7 (9)	C1R3–C2R3–C3R3	120.5 (10)
C2R1–C3R1–C4R1	120.9 (9)	C2R3–C3R3–C4R3	120.0 (10)
C3R1–C4R1–C5R1	120.6 (9)	C3R3–C4R3–C5R3	120.2 (11)
C4R1–C5R1–C6R1	118.0 (9)	C4R3–C5R3–C6R3	119.8 (10)
C5R1–C6R1–C1R1	122.5 (8)	C5R3–C6R3–C1R3	120.3 (10)
C6R1–C1R1–C2R1	119.1 (8)	C6R3–C1R3–C2R3	118.6 (10)
C1R2–C2R2–C3R2	120.6 (9)	C1R4–C2R4–C3R4	120.5 (9)
C2R2–C3R2–C4R2	115.5 (10)	C2R4–C3R4–C4R4	115.5 (10)
C3R2–C4R2–C5R2	129.0 (12)	C3R4–C4R4–C5R4	126.8 (11)
C4R2–C5R2–C6R2	115.9 (11)	C4R4–C5R4–C6R4	116.8 (11)
C5R2–C6R2–C1R2	120.0 (10)	C5R4–C6R4–C1R4	121.2 (10)
C6R2–C1R2–C2R2	118.8 (9)	C6R4–C1R4–C2R4	119.3 (9)
		mean	120.0
C1B–C2B	1.38 (2)	C1B–C2B–C3B	104.4 (18)
C2B–C3B	1.41 (2)	C2B–C3B–C4B	136.3 (21)
C3B–C4B	1.41 (2)	C3B–C4B–C5B	112.1 (20)
C4B–C5B	1.48 (2)	C4B–C5B–C6B	117.1 (21)
C5B–C6B	1.45 (2)	C5B–C6B–C1B	118.7 (20)
C6B–C1B	1.42 (2)	C6B–C1B–C2B	130.4 (19)
mean	1.425	mean	119.8
C1Et–C2Et	1.48 (3)	C1Et–C2Et–O1Et	131.8 (27)
C2Et–O1Et	1.39 (3)		

[a] The solvent values are discussed in the text.

metalloporphyrins, the region below the plane of the porphyrin, opposite the axial pyridine, is vacant. The closest approach to the zinc in this position is the Zn–H contact of 3.4 Å between the metal and a proton on phenyl ring 3 of a symmetry-related porphyrin.

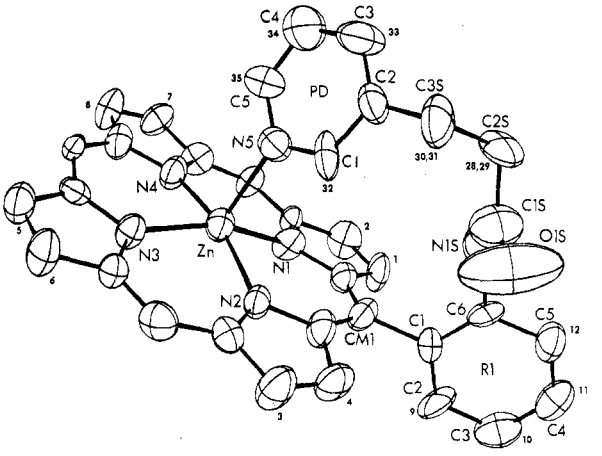

Figure 3. A view of **1** showing the side arm conformation and atomic numbering. (Hydrogens bonded to the three omitted phenyl rings are numbered 13–27 in a manner analogous to the numbering of phenyl ring 1.)

Discussion

Zinc Coordination Sphere. The coordination geometry about zinc is striking in its similarity to the structure of the closely related [5,10,15,20-tetrakis(4-pyridyl)porphinato](pyridine)-zinc(II).[19] In the present study, zinc–porphyrin nitrogen bond lengths are 2.052 (7)–2.074 (7) Å; for the previously reported compound,[19] values of 2.067 (3) and 2.079 (2) Å were obtained for these distances. The zinc–pyridine nitrogen distance for the present compound is 2.147 (7) Å; for the previously reported compound,[19] this value is 2.143 (4) Å. In the previously reported compound,[19] the zinc is displaced out of the porphyrin plane toward the axial ligand by 0.33 Å. For compound **1**, a value of 0.37 Å is found. The close agreement between zinc–pyridine nitrogen distance and zinc out-of-plane distance may argue against much steric strain or bond elongation in the zinc–pyridine region due to covalent attachment of a pyridine to the porphyrin ring, at least with the four-atom connecting chain present in this compound. A minor steric effect of covalent attachment is a very slight tipping of the pyridine ring along the Zn–N5 axis such that the one α proton

Table V. Best-Weighted Least-Squares Planes for ZnTPP-NHC(O)$CH_2CH_2C_5H_4N$ [$Ax + By + Cz - D = 0$ (Orthogonalized Coordinates, Å)]

plane no.	atoms in planes	*A*	*B*	*C*	*D*
1	N1, N2, N3, N4, C1P1, C2P1, C3P1, C4P1, C1P2, C2P2, C3P2, C4P2, C1P3, C2P3, C3P3, C4P3, C1P4, C2P4, C3P4, C4P4, CM1, CM2, CM3, CM4[a]	−0.3198	0.0262	−0.9484	−6.2070
2	N1(7,7),[b] C1P1(−3,9), C2P1(−9,10), C3P1(19,10), C4P1(−18,9)	−0.1861	0.0196	−0.9823	−6.9165
3	N2(2,8), C1P2(−7,9), C2P2(−9,11), C3P2(−5,10), C4P2(0,10)	−0.4132	0.0872	−0.9065	−5.7671
4	N3(−7,7), C1P3(5,9), C2P3(4,11), C3P3(−13,11), C4P3(14,10)	−0.4053	0.0254	−0.9138	−5.7780
5	N4(5,7), C1P4(0,10), C2P4(−9,10), C3P4(15,11), C4P4(−13,10)	−0.2491	−0.0539	−0.9670	−6.6477
6	N5(−4,9), C1PD(7,12), C2PD(1,12), C3PD(−11,14), C4PD(10,15), C5PD(1,14)	0.6011	−0.7989	−0.0192	−1.8698
7	C1R1(20,11), C2R1(−9,14), C3R1(−11,14), C4R1(11,13), C5R1(6,14), C6R1(−21,13)	0.9249	−0.2572	−0.2802	−4.6450
8	C1R2(−7,12), C2R2(12,14), C3R2(−1,15), C4R2(−17,15), C5R2(21,16), C6R2(−5,15)	0.0598	0.9238	−0.3782	−2.5481
9	C1R3(−25,12), C2R3(43,15), C3R3(−8,15), C4R3(−38,15), C5R3(45,15), C6R3(−6,14)	0.9227	−0.2609	−0.2838	−4.5765
10	C1R4(−12,12), C2R4(5,13), C3R4(4,15), C4R4(−3,15), C5R4(−9,16), C6R4(17,15)	−0.3339	−0.9426	−0.0018	0.6011
11	Zn, N1, N3, N5	0.8223	0.4998	−0.2720	−3.8221
12	Zn, N2, N4, N5	0.4914	−0.8639	−0.1101	−2.6033
13	Zn(0,1), N5(36,9), C1PD(−24,12), C5PD(−30,14)	0.5762	−0.8089	−0.1173	−2.8325

planes	dihedral angle, deg	planes	dihedral angle, deg	planes	dihedral angle, deg	planes	dihedral angle, deg
1-2	7.9	1-6	101.0	1-10	84.9	11-12	89.9
1-3	7.0	1-7	92.1	1-11	89.7	11-13	84.2
1-4	5.3	1-8	69.0	1-12	94.1	12-13	5.8
1-5	6.0	1-9	91.8	1-13	95.2		

[a] Deviations of these atoms from plane 1 are illustrated in Figure 1. [b] Distances from the planes and standard deviations of these values are given in parentheses for each atom. Units are Å × 10^{-3}.

Table VI. Root-Mean-Square Amplitudes of Thermal Vibration (Å)

atom	min	intermed	max
Zn	0.183	0.223	0.226
N1	0.133	0.218	0.260
N2	0.160	0.203	0.232
N3	0.172	0.198	0.236
N4	0.174	0.232	0.245
N5	0.204	0.215	0.268
C1P1	0.169	0.205	0.257
C2P1	0.141	0.260	0.302
C3P1	0.210	0.246	0.293
C4P1	0.145	0.196	0.276
C1P2	0.183	0.217	0.222
C2P2	0.202	0.233	0.331
C3P2	0.169	0.255	0.287
C4P2	0.173	0.224	0.265
C1P3	0.160	0.188	0.274
C2P3	0.183	0.245	0.275
C3P3	0.184	0.252	0.303
C4P3	0.182	0.205	0.251
C1P4	0.181	0.221	0.250
C2P4	0.159	0.269	0.281
C3P4	0.176	0.248	0.313
C4P4	0.169	0.185	0.300
CM1	0.172	0.231	0.252
CM2	0.183	0.241	0.251
CM3	0.129	0.178	0.276
CM4	0.177	0.198	0.255
C1R1	0.148	0.228	0.239
C2R1	0.132	0.279	0.307
C3R1	0.166	0.292	0.323
C4R1	0.184	0.271	0.303
C5R1	0.182	0.236	0.311
C6R1	0.100	0.258	0.281
N1S	0.213	0.256	0.366
C1S	0.190	0.312	0.337
O1S	0.263	0.302	0.654
C2S	0.218	0.252	0.361
C3S	0.191	0.242	0.353
C1PD	0.194	0.243	0.259
C2PD	0.131	0.213	0.303
C3PD	0.147	0.296	0.369
C4PD	0.233	0.264	0.402
C5PD	0.221	0.255	0.332

(H32) is slightly closer (0.04 Å) to the porphyrin ring (N2) than is the other α proton (H35) to the ring (N4). This positioning of H32 or α'-H closer to the porphyrin ring than is H35 or α-H may explain why the NMR resonance[14] of the former is upfield from that of the latter for compound **1** and its three-atom side-chain analogue, but the relative positions of the resonances of α'-H and α-H reverse on going to longer chain analogues,[14] since the position of these NMR resonances is strongly affected by the distance of the proton from the porphyrin ring current.[53]

Conformation and Bonding Effect of the Side-Arm Connecting Link. The covalent attachment of the axial pyridine in compound **1** produces a 13-membered chelate ring. Although under normal circumstances such a large potential chelate ring would not lead to thermodynamically favorable binding of the donor atom to the same metal to which the rest of the ligand system is bound, the geometrical constraints imposed by the porphyrin, phenyl, and pyridyl ring atom members of this 13-membered ring require the pyridyl to bind only to its own zinc. No evidence is found in the NMR spectra of **1** or its longer side-arm analogues to suggest that the pyridyl group binds to other than its own zinc atom,[14] and certainly the present structure and the relationship of the individual molecules within the unit cell indicate the strong preference of the side-arm pyridyl for its own zinc.

The side arm imposes chirality upon the molecular structure of **1**, and the unit cell contains two enantiomeric pairs in symmetry-related positions. N1S is directly above C1R1 while C1S and O1S are above but angled away from the plane of the phenyl ring to which the side arm is attached. This positioning determines the direction of rotation of the pyridine ring in the enantiomeric units.

Bond angles within the side arm show some distortion from their expected values. For example, at the amide carbonyl carbon, the C2S–C1S–N1S angle is only 115.1 (12)°. At the formally tetrahedral carbons C2S and C3S, the angles are found to be somewhat larger, 112.9 (8) and 113.2 (8)°, respectively. These values suggest that the absence of abnormal distances in the immediate zinc coordination sphere is compensated in part by distortion within the covalent attachment.

In the thermodynamic study of side-arm ligand replacement by 3-picoline,[14] compound **1** was found to form a weaker $Zn-N_{py}$ bond than its longer side-arm analogues, and this was attributed to steric strain of the Zn–N bond produced by the short (four-atom) connection between the pyridyl and phenyl rings. It is now apparent that this steric strain manifests itself not in the immediate coordination sphere of zinc but rather in the atoms of the connecting chain and in the conformation of the porphyrin.

The contacts between the atoms of the side arm and the porphyrin ring are minimal; the closest nonbonding contact is between the ring and a hydrogen on C2S (~2.6 Å). The amide nitrogen N1S is 2.9 Å from CM1, and directly above C1R1, and the other atoms of the amide linkage are more than 3 Å away from the porphyrin ring. This would seem to preclude any direct through-space electronic interaction between the amide group and the porphyrin π system, as has been suggested from thermodynamic[14] and electrochemical[54] studies of **1** and its analogues. However, it must also be noted that the π-electron density of the porphyrin ring apparently extends somewhat outside the meso carbon atom position, as is evidenced by the fact that the NMR resonances of the ortho phenyl protons in Ni(II)[55] and Zn(II)[14,55] and other diamagnetic metallotetraphenylporphyrins[56] are always shifted downfield about 1 ppm from their nonporphyrinic phenyl positions (and about 0.5 ppm downfield of their meta and para phenyl prophyrin counterparts) and thus are outside the π-electron ring, which gives rise to a deshielding ring current effect.[53] In contrast, the methyl protons of tetra-*o*-tolylmetalloporphyrins are shifted upfield about 0.6–0.7 ppm from their tetra-*m*-tolyl and tetra-*p*-tolyl analogues,[55,56] and thus the protons of the ortho methyl substituent are well inside or within the π-electron ring, which gives rise to a shielding ring current effect.[53] Perhaps the amide nitrogen and oxygen are close enough when the molecule has more freedom of motion in solution to give rise to the observed electron-withdrawing enthalpy effect observed in thermodynamics of axial-ligand displacement[14] and the third oxidation peak observed in cyclic voltammetric studies[54] of **1** and its analogues, which is in addition to the formation of mono- and dication radicals for ZnTPP. In CH_2Cl_2 this third oxidation occurs at about 1.4 V vs. SCE.[54]

Orientation of the Pyridine Ligand. As discussed previously, one of the reasons for incorporating a covalent linkage between the porphyrin moiety and an axial ligand is to obtain control over the orientation of the axial ligand ring (or rings) with respect to the porphyrin nitrogens. As a first step in this overall plan, if tetraphenylporphyrins are to be used, one must design

(53) R. J. Abraham, A. H. Jackson, G. W. Kenner, and D. Warburton, *J. Chem. Soc.*, 853 (1963); C. B. Storm and A. H. Corwin, *J. Org. Chem.*, **29**, 3700 (1964); R. J. Abraham, *Mol. Phys.*, **4**, 145 (1961); A. R. Kane, R. G. Yalman, and M. E. Kenney, *Inorg. Chem.*, **7**, 2588 (1968).

(54) F. A. Walker and M. Z. Wu, unpublished work.

(55) F. A. Walker and G. L. Avery, *Tetrahedron Lett.*, **52**, 4949 (1971).

(56) F. A. Walker and T. Tom, unpublished work.

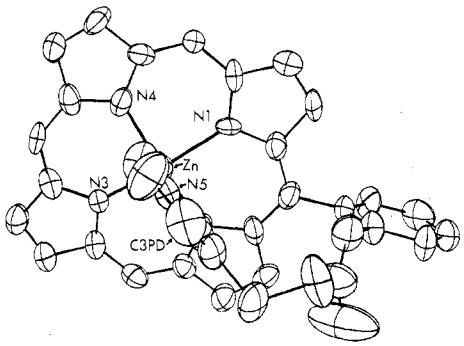

Figure 4. An ORTEP plot of **1** seen in the same orientation as in Figure 1 illustrating the alignment of the pyridine ring and the conformation of the covalent linkage.

a linkage short enough to ensure that the axial ligand ring is aligned between (rather than directly above) the porphyrin nitrogens. Molecular models (CPK) strongly implied that the side arm used in the present compound, a four-atom chain, would be sufficiently short and the pyridine ring would lie between the porphyrin nitrogens. That is, the dihedral angle between the plane defined by the axial pyridine and a plane defined by the zinc and either pair of diagonally opposed in-plane nitrogens was expected to be very close to 45°. Predictions based on molecular models notwithstanding, it has been determined in this study that the pyridine is aligned almost directly above two opposite porphyrin nitrogens. Table V lists pertinent best-weighted least-squares planes and dihedral angles. The dihedral angle between the plane defined by Zn, N2, N4, and N5 and that determined by Zn, N5, C1PD, and C5PD is 5.8°. This is illustrated in Figure 4. In strong contrast to this, in [5,10,15,20-tetrakis(4-pyridyl)porphinato](pyridine)zinc(II),[19] the comparable dihedral angle is 22.8°.

In the other report[15] of the structure of a metalloporphyrin with a covalently attached axial ligand, the axial ligand plane was also rotated to an angle of about 4° with respect to N2 and N4. However, the connecting chain contained two additional atoms in that covalently attached (imidazole)(tetraphenylporphyrin)iron–thioether complex, and such a long chain could well accommodate a fairly high degree of freedom of rotation about the $Fe-N_{Im}$ bond.

The observed conformation of the pyridine is the least expected one and, as was discussed earlier, the one most susceptible to considerable strain. In summary, compound **1** relieves this strain in the following ways: (i) the zinc is displaced from the plane by 0.37 Å; (ii) the pyridine ligand is tilted slightly toward the covalent chain; (iii) C–C single bond angles are found to be larger than expected in the chain; (iv) the phenyl bearing the chain is tipped ~7° toward the pyridine ligand; (v) the methine carbon to which this phenyl group is bonded is displaced above the mean porphyrin plane by 0.24 Å.

The results of this study of the solid-state structure of **1** strongly imply that, for this chain length, the pyridine is most likely capable of rotating ca. 80° about the N5–Zn axis in solutions of **1**. Although such rigid structural control was not required or even desired in the previously reported study of covalently attached axial-ligand displacement from a series of 5-coordinate zinc side arm porphyrins,[14] it is a necessity for our desired goal of producing models of the cytochromes *b* in which the two axial imidazoles are aligned with the projection of their molecular planes on the porphyrin ring mutually parallel and mutually perpendicular.[16] Thus, it would appear that such rigid structural control can only be obtained by using shorter than four-atom connecting chains. However, the present 5-coordinate structure contains one feature which is not expected to be present in the 6-coordinate cytochrome *b* models: the metal atom is displaced 0.37 Å out of the plane of the porphyrin ring toward the axial ligand. What effect the in-plane positioning of a metal atom will have on the angular orientation of axial ligands remains to be discovered from solution and solid-state structural studies in progress.

Acknowledgment. Support of this work by the National Science Foundation (Grants CHE-75-20123 and 79-18217) and National Institutes of Health in the form of a Research Career Development Award (5K04 GM 00227) (F.A.W) is gratefully acknowledged. The authors thank Professor Keith O. Hodgson of Stanford University for access to the X-ray Crystallographic Facility and for discussions concerning the ethanol disorder. M.A.B. acknowledges the technical assistance of Mr. Jeremy Berg and Dr. Thomas Wolff during the final refinement cycles.

Registry No. **1**, 74552-67-3.

Supplementary Material Available: Table VII giving calculated hydrogen positions, Table VIII giving general temperature factor expressing, *B*'s and *U*'s, and Table IX giving values of $10|F_o|$ and $10|F_c|$ (22 pages). Ordering information is given on any current masthead page.